Journal of Nuclear Medicine, published on October 30, 2017 as doi:10.2967/jnumed.117.197624

Manuscript Title: Prospective Evaluation of ^{68}Ga-RM2 PET/MRI in Patients with Biochemical Recurrence of Prostate Cancer and Negative Conventional Imaging

Authors: Ryogo Minamimoto[1], MD; Ida Sonni, MD[1]; Steven Hancock, MD[2]; Shreyas Vasanawala, MD, PhD[3]; Andreas Loening, MD[3], PhD; Sanjiv S. Gambhir, MD[4,5,6], PhD; Andrei Iagaru, MD[1]

[1] Department of Radiology, Division of Nuclear Medicine and Molecular Imaging, Stanford University

[2] Department of Radiation Oncology, Stanford University

[3] Department of Radiology, Radiological Sciences Laboratory, Stanford University

[4] Department of Radiology, Stanford University

[5] Department of Bioengineering, Stanford University

[6] Department of Materials Science and Engineering, Stanford University

Corresponding author: Andrei Iagaru, MD

Department of Radiology

Division of Nuclear Medicine and Molecular Imaging

Stanford University

300 Pasteur Dr, Room H-2200

Stanford, CA 94305 USA

Phone: 650 725 4711

Fax: 650 498 5047

Email: aiagaru@stanford.edu

Manuscript type: original research

Running title: ^{68}Ga-RM2 PET/MRI in Prostate Cancer

Words count: 4871

ClinicalTrials.gov Identifier: NCT02624518

Key words: prostate cancer; ^{68}Ga; RM2; gastrin-releasing peptide receptors (GRPr); PET/MRI

ABSTRACT

Purpose: ^{68}Ga-labeled DOTA-4-amino-1-carboxymethyl-piperidine-D-Phe-Gln-Trp-Ala-Val-Gly-His-Sta-Leu-NH2 (^{68}Ga-RM2) is a synthetic bombesin receptor antagonist that targets gastrin-releasing peptide receptors (GRPr). GRPr proteins are highly overexpressed in several human tumors, including prostate cancer. We present data from the use of ^{68}Ga-RM2 in patients with biochemical recurrence (BCR) of prostate cancer (PCa) and negative conventional imaging (CI).

Methods: We enrolled 32 men with BCR PCa, 59-83 year-old (mean±standard deviation (SD): 68.7±6.4). Imaging started at 40-69 minutes (mean±SD: 50.5±6.8) after injection of 133.2-151.7 MBq (mean±SD: 140.6±7.4) of ^{68}Ga-RM2 using a time-of-flight (TOF)-enabled simultaneous positron emission tomography (PET) / magnetic resonance imaging (MRI) scanner. T1-weighted (T1w), T2-weighted (T2w) and diffusion-weighted images (DWI) were acquired.

Results: All patients had rising prostate specific antigen (PSA) (range: 0.3-119.0 ng/mL; mean±SD: 10.1 ± 21.3) and negative CI (CT or MRI, and ^{99m}Tc MDP bone scan) prior to enrollment. The observed ^{68}Ga-RM2 PET detection rate was 71.8%. ^{68}Ga-RM2 PET identified recurrent PCa in 23 of the 32 participants, while the simultaneous MRI scan identified findings compatible with recurrent PCa in 11 of the 32 patients. PSA velocity (PSAv) values were 0.32±0.59 ng/ml/year (range: 0.04-1.9) in patients with negative PET scans and 2.51±2.16 ng/ml/year (range: 0.13-8.68) in patients with positive PET scans (*P*: 0.006).

Conclusions: ^{68}Ga-RM2 PET can be used for assessment of GRPr expression in patients with BCR PCa. High uptake in multiple areas compatible with cancer lesions suggests that ^{68}Ga-RM2 is a promising PET radiopharmaceutical for localization of disease in participants with BCR PCa and negative CI.

INTRODUCTION

Up to 40% of the patients with PCa develop BCR within 10 years after initial treatment (*1*). A detectable or rising PSA level after initial therapy is considered BCR or "PSA failure", even when there are no symptoms or signs of locally recurrent or metastatic disease (*2*). Usually an increase of the PSA level precedes a clinically detectable recurrence by months to years (*3*). However, it cannot differentiate between local, regional or systemic disease with the necessary precision that is essential for further disease management.

Morphological imaging methods exhibit considerable limitations: sensitivity ranges between 25% and 54% for the detection of local recurrence by trans-rectal ultrasound or contrast-enhanced CT and is moderately improved by using functional MRI techniques (*4*). The sensitivity for detection of lymph node metastases of CT or MRI is reported to be 30-80% (*5*). Multi-parametric MRI (mpMRI) is improving PCa diagnosis (*6*). Using a scoring system based on a combined evaluation of DWI, dynamic contrast-enhanced MRI, and high-resolution T2w imaging (*7*), the degree of suspicion on MRI strongly correlates with the presence of PCa. However, mpMRI has limitations: ~20% of all index lesions are missed *(8)*, the size of high grade cancers is undersestimated *(9)*, and ~40% of men with a normal MRI have PCa on biopsy *(10)*.

Molecular imaging uses various targets to improve the detection of recurrent PCa. ^{18}F- or ^{11}C-labeled choline and ^{11}C-acetate were investigated (*11-13*). ^{18}F-FACBC was recently approved for the detection of PCa recurrence and tracers binding to the prostate-specific membrane antigen (PSMA) continue to elicit high interest, although none are yet approved by the Food and Drug Administration. These promising agents do not detect all recurrences (*14,15*) and are not specific to PCa only (*16,17*). False positives have also been reported (*18-20*).

Consequently, improved imaging of BCR PCa continues to be an area of unmet clinical need. ^{68}Ga-RM2 is a synthetic bombesin receptor antagonist that targets GRPr (*21*). GRPr are highly overexpressed in several human tumors, including PCa (*22*). GRPr was detected in 63-100% of PCa (*23*,*24*). Due to their low expression in benign prostate hypertrophy and inflammation (*24*), imaging GRPr has potential advantages over other radiopharmaceuticals. In a first pilot study comparing ^{68}Ga-RM2 to ^{68}Ga-PSMA-11 in PCa, both compounds performed very well (*25*).

PET/MRI is an advanced technology that provides both biological and morphological information, with improvements over PET/CT due to better soft tissue contrast (*26*). In this study we evaluated ^{68}Ga-RM2 in patients with BCR PCa and negative CI, using a state-of-the-art TOF-enabled simultaneous PET/MRI scanner.

MATERIALS AND METHODS

Study Population

The local Institutional Review Board and the Stanford Cancer Institute Scientific Review Committee approved the protocol. Written informed consent was obtained from all patients before participation in the study.

Inclusion Criteria

1) Biopsy proven PCa

2) Rising PSA after definitive therapy with prostatectomy or radiation therapy (external beam or brachytherapy)

- Post radical prostatectomy – American Urological Association recommendation (*27*)
    i. PSA greater or equal to 0.2 ng/mL measured after at least 6 weeks from

radical prostatectomy

ii. Confirmatory persistent PSA greater than or equal to 0.2 ng/mL (total of two PSA measurements greater than 0.2 ng/mL)

- Post radiation therapy – American Society for Radiation Oncology-Phoenix consensus definition (*28*)

i. A rise of PSA measurement of 2 or more ng/mL over the nadir

3) No evidence of metastatic disease on CI, including a negative bone scan for skeletal metastasis and negative contrast-enhanced CT or MRI;

4) Able to provide written consent

5) Karnofsky performance status of ≥50 (or ECOG/WHO equivalent).

Exclusion Criteria:

1) Less than 18 years-old at the time of radiotracer administration;

2) Unable to provide informed consent;

3) Inability to lie still for the entire imaging time;

4) Inability to complete the needed investigational and standard-of-care imaging examinations due to other reasons (severe claustrophobia, radiation phobia, etc.);

5) Any additional medical condition, serious intercurrent illness, or other extenuating circumstance that, in the opinion of the Investigator, may significantly interfere with study compliance

6) Metallic implants (contraindicated for MRI).

Preparation of ^{68}Ga-RM2

The precursor, DOTA-4-amino-1-carboxymethylpiperidine-*D*-Phe-Gln-Trp-Ala-Val-Gly-His-Sta-Leu-NH_2 (DOTA-RM2), was obtained from ABX GmbH (Radeberg, Germany). A ^{68}Ga-

labeling kit including eluent (concentrated NaCl/HCl solution), sodium acetate reaction buffer, ethanol (50% in water) and saline (0.9%) was obtained from Eckert & Ziegler Eurotope GmbH (Berlin, Germany). Phosphate buffer concentrate (1 M Na^+, 0.6 M PO_4^{3-}) for pH adjustment was obtained from B. Braun (Melsungen, Germany).

The radiosynthesis was conducted with a fully automated synthesis device (Modular Lab PharmTracer, Eckert & Ziegler Eurotope GmbH) using sterile single-use cassettes, as previously reported (*25*).

PET/MRI Protocol

No specific patient preparation such as fasting or hydration was required prior to the ^{68}Ga-RM2 scans. Imaging (vertex to mid-thighs) started at 40-69 minutes (mean±SD: 50.5±6.8) after injection of 133.2-151.7 MBq (mean±SD: 140.6±7.4) of ^{68}Ga-RM2 using a TOF-enabled simultaneous PET/MRI scanner (SIGNA PET/MR, GE Healthcare, Waukesha, WI, USA). The range of time from injection to start of imaging is similar to guidelines recommendations for other radiopharmaceuticals evaluating PCa (*29*). The duration of the scan ranged 39-141 minutes (mean ± SD: 76.1±17.4). The range is due mostly to the fact that the duration of exam is directly related to the patient's height. The height ranged from 5'4" to 6'1" as detailed in Supplemental Table 1. In addition, one patient was not able to tolerate the entire duration of exam. The PET acquisition was performed in 3D mode and 4 minutes/bed position (89 slices/bed) in 5-9 beds. An axial 2-point Dixon 3D T1w spoiled gradient echo MR sequence was acquired at each table position and used to generate attenuation correction maps and for anatomic registration of the PET results. PET images were reconstructed using ordered subset expectation maximization protocol with 2 iterations and 28 subsets. TOF reconstructed images assumed a Gaussian kernel of 400 ps width. The Dixon MRI sequence and the PET acquisition started at the same table position and times, thus ensuring optimal temporal and regional correspondence between MRI

and PET data. For attenuation correction, the images were segmented into different tissue types with an anatomy-aware algorithm, and were co-registered to a CT atlas in the head region (*30*).

Additional sequences acquired at each station included: coronal T2w single-shot fast spin echo with variable refocusing flip angles and outer volume suppression (*31*), coronal DWI and axial T1w 2-point Dixon 3D spoiled gradient echo. Spectral inversion at lipids fat suppression was applied at every other station. Because of the large prescribed field of view, each acquisition covered two consecutive beds allowing T2w whole-body images with and without fat suppression to be retrospectively generated. Coronal DWI was performed using a custom-developed 2D single-shot echo planar imaging sequence, with 2D spatial selectivity obtained by replacing the conventional spectral-spatial excitation pulse with a 2D radiofrequency pulse. T1w images were acquired using an axial 2-point Dixon 3D gradient echo sequence provided by the manufacturer (LAVA-flex). In the thorax region, the MRI scans were acquired during a breath-hold in shallow inspiration except for DWI, which was always performed during free breathing.

Image Analysis

Two board certified Nuclear Medicine physicians (AI, RM) with 12 and 7 years experience interpreting PET studies, respectively, reviewed PET images using MIMvista version 6.2 (MIMvista Corp, Cleveland, OH, USA). All areas of increased radiotracer uptake in sites not expected to show physiological accumulation were reported as “abnormal”. Increased uptake was defined as focal tracer uptake higher than adjacent background. ^{68}Ga-RM2 uptake was considered as physiological in the following tissues: gastrointestinal tract, liver, spleen, pancreas, kidneys, ureters, bladder. This approach is similar to recently published guidelines for standard image interpretation developed for ^{68}Ga PSMA image interpretation (*32*). The PETedge tool available in the software was used for evaluation of focal ^{68}Ga-RM2 uptake outside the expected

biodistribution. The diameter of anatomical structures corresponding to focal ^{68}Ga-RM2 uptake were measured on T1w MR images.

Two board certified radiologists (AML, SSV, 5 and 11 years experience interpreting body MRI studies, respectively) evaluated the MR images for detection of areas of abnormal signal or anatomical structures, blinded to the results of PET or other studies. Visual conspicuity against background on the diffusion weighted images and presence of an anatomically corresponding abnormality on the T1w and T2w images were the criteria for detecting a lesion on MRI.

RESULTS

We enrolled 32 men with BCR PCa, 59-83 year-old (mean±SD: 68.7±6.4). Patients had multiple standard of care imaging studies (CT, MRI, ^{18}F NaF PET/CT, ^{99m}Tc MDP bone scan - as shown in Supplemental Table 1) prior to enrollment that were negative, despite rising PSA values from nadir. The order of the standard of care imaging studies was not controlled and the interval between bone scan and anatomic imaging ranged 0-28 days (mean ± SD: 3.5±7.1). The time from CI to enrollment in the protocol ranged 1-45 days (mean ± SD: 26.7±12.7). The patients did not receive treatment in this interval. The interval from BCR to the ^{68}Ga-RM2 PET/MRI scan ranged 1-75 months (mean ± SD: 21.8±19.5).

Patient characteristics are shown in Supplemental Table 1, while results of PET/MRI and follow-up data are shown in Supplemental Table 2. Patients were not treated for PCa at the time of enrollment in the protocol. All patients tolerated the procedure without immediate or delayed (up to 7 days) complaints or complications. The biodistribution of ^{68}Ga-RM2 is similar to

previous reports (*33*,*34*).

^{68}Ga-RM2 Uptake Outside the Expected Physiologic Biodistribution

Nine scans had no focal ^{68}Ga-RM2 uptake outside the expected physiologic biodistribution. The remaining 23 patients had high focal ^{68}Ga-RM2 uptake that corresponded on MRI to retroperitoneal lymph nodes, bone marrow, mediastinal lymph nodes, pelvic lymph nodes, seminal vesicle, supraclavicular lymph nodes, mesenteric lymph nodes, liver, lung and prostate bed on MRI. These areas of high ^{68}Ga-RM2 uptake had SUV_{max} of 13.4±8.3 (range: 2.6-33.5) and SUV_{mean} of 6.7±3.9 (range: 1.7-16.1), above the background and easily identifiable given the minimal hepato-biliary clearance. The mean diameter of lymph nodes with high ^{68}Ga-RM2 uptake was 1.3±0.8 cm (range: 0.4-2.9 cm).

Participants were followed for an average of 17.1±5.2 month (range 3-25 month) after ^{68}Ga-RM2 scan. Of the 23 participants with findings on ^{68}Ga-RM2 PET, 20 began treatment. Two participants continued active surveillance and a third declined offered treatment. In total, 7 of the 23 ^{68}Ga-RM2 positive cases had biopsies that confirmed the PET findings. Conversely, of the 9 participants with no findings on ^{68}Ga-RM2 PET, 6 continued on active surveillance, 2 received treatment and 1 was lost to follow-up. Participants with findings on ^{68}Ga-RM2 PET undergoing immediate active treatment in general had a decrease in their PSA measurments, while patients who initially remained under observation had an increase in their PSA and started treatment. All these are detailed in Supplemental Table 2.

Relationship Between PSA Measurements and Results of the Scan

PSA values were sampled 21.4±10.8 days (range: 1-30 days) prior to the scan and measured 10.1±21.3 ng/ml (range: 0.3-119.0). PSA values were 2.4±2.5 ng/ml (range: 0.3-6.7) in

patients with negative PET scans and 13.2±24.5 ng/ml (range: 1.1-119.0) in patients with positive PET scans. This difference was not statistically significant (*P*: 0.20). Figure 1 shows the results in relationship of scan positivity to PSA values and PSAv.

Relationship Between PSAv and Results of the Scan

PSAv measured 1.89±2.1 ng/ml/year (range: 0.04-8.68). PSAv values were 0.32±0.59 ng/ml/year (range: 0.04-1.9) in patients with negative PET scans and 2.51±2.16 ng/ml/year (range: 0.13-8.68) in patients with positive PET scans. This difference was statistically significant (*P*: 0.006). Of the nine patients with negative ^{68}Ga-RM2 scans only 1 patient had a PSAv >0.3 ng/ml/year.

MRI Findings

Eleven of the 32 participants had findings compatible with recurrent PCa on the MRI component of PET/MRI. These included lymph nodes, prostate bed, lung and bone marrow lesions. All were also positive on ^{68}Ga-RM2 PET. The remaining 21 participants had no abnormal findings identified prospectively.

Examples of recurrent PCa are shown in Figures 2-5.

DISCUSSION

Our study is the largest to date to prospectively evaluate ^{68}Ga-RM2 in a series of patients with BCR PCa. In this population with mean PSA of 10.1 ng/mL the ^{68}Ga-RM2 PET observed detection rate was 71.8%. ^{68}Ga-RM2 PET/MRI showed intense uptake in multiple subcentimeter pelvic/retroperitoneal/mesenteric lymph nodes, as well as in prostate bed, seminal vesicle, lungs, liver and bone marrow lesions that had not been identified by CI done **prior** to enrollment in our

protocol. However, some of the lesions such as lung nodules were outside the standard field of view for restaging PCa when using anatomical imaging. The high uptake in pancreas and moderate uptake in the gastrointestinal tract are specific features of ^{68}Ga-RM2 biodistribution. The pancreas and gastrointestinal tract express GRPr (*35*) and bombesin works as a stimulator of pancreatic secretion, as well as gastrin and cholecystokinin release (*36*,*37*). ^{68}Ga-RM2 PET identified recurrent PCa in 23 of the 32 participants (71%), while the simultaneous MRI scan identified findings compatible with recurrent PCa in only 11 of the 32 patients (34%). Of the nine RM2 negative patients, 2 had no evidence of disease throughout the follow-up period, 1 was lost to follow-up and determination of clinical disease was not possible, and 6 were false negative in patients with subsequent clinical disease. The percentage of patients with a correct diagnosis (compared to clinical outcome) was 80.1% (25/31). The confirmed false negative was thus 16.1% (5/31). All of the RM2 false negative patients were also false negative by MRI. There were no patients with clinical disease who had a positive MRI scan and a negative RM2 scan.

Our results indicate that PSAv may be a tool to decide which patients may have positive ^{68}Ga-RM2 PET, with a statistically significant difference in PSAv between those with negative and positive ^{68}Ga-RM2 PET. The mean PSAv of 0.32±0.59 ng/ml/year (median: 0.14) in patients with negative PET scans and 2.50±2.21 ng/ml/year (median 1.95) reveals a significant difference in the pathology and potential prognosis in patients with lesions visualized by ^{68}Ga-RM2 PET. It should be noted that the mean value of PSAv was >2 ng/ml/year in participants with positive ^{68}Ga-RM2 PET. A PSAv greater than 2.0 ng/ml/year was significantly associated with a shorter time to PCa-specific mortality and all-cause mortality when compared with men whose PSAv was 2.0 ng/ml/year or less (*38*). If corroborated in a larger study, a negative ^{68}Ga-RM2 scan,

even in the face of an elevated PSA may indicate a patient with a relatively benign prognosis in which a watch and wait strategy is indicated. Our preliminary follow-up data shown in Supplemental Table 2 would support this hypothesis.

To date only 3 studies reported the performance of ^{68}Ga-RM2 PET in BCR PCa. Kähkönen et al. evaluated ^{68}Ga-RM2 in 14 men with prostate cancer using PET/CT; however, 11 of the 14 participants had the scans done for evaluation at initial diagnosis and only 3 of the 14 were scanned at BCR. In their study, the sensitivity for detection of primary PCa was 88% and for lymph node metastases was 70% (*34*). Other GRPr targeting PET radiopharmaceuticals have been recently reported in small cohorts, illustrating the attractiveness of this target for detection of PCa. Maina and colleagues evaluated ^{68}Ga-SB3 in 8 patients with breast cancer and 9 patients with PCa (*39*). ^{68}Ga SB3 did not produce adverse effects and identified cancer lesions in 4 out of 8 (50 %) with breast cancer and 5 out of 9 (55 %) with PCa. An improved version of this radiopharmaceutical, ^{68}Ga NeoBOMB1, is showing promising results in preliminary studies (*40*,*41*).

In our study, ^{68}Ga-RM2 showed high focal uptake in small lymph nodes that had no MRI features compatible with metastatic disease. Future larger studies will compare ^{68}Ga-RM2, mpMRI and/or one of the new PSMA PET radiopharmaceuticals for the detection of metastatic PCa. The high performance of the TOF-enabled PET/MRI scanner (*30*) likely contributed to the identification of focal ^{68}Ga-RM2 uptake in structures of non-pathologically increased size but outside the expected physiologic ^{68}Ga-RM2 biodistribution. However, if there is no concern for pelvic recurrence, the use of PET/CT scanner is likely to yield similar results to PET/MRI with faster imaging times, especially when using recently introduced SiPM-based PET/CT scanners (*42*).

One of the limitations of our study is the small number of patients. Another limitation is the lack of correlation with pathology results for all patients; despite this, histopathological correlation was available in approximately 1/3 of those with findings on ^{68}Ga-RM2 PET. Pathology was available in 7 out of 23 patients with findings on ^{68}Ga-RM2 PET and all 7 were confirmed to represent recurrent PCa. Given the small size of many of the lymph nodes with focal uptake, accurate sampling would not have been feasible in all cases. Another limitation is the heterogeneity of the PSA values and the prior treatment regimens at the time of enrollment in the study; however, this is expected in early evaluations of new radiopharmaceuticals. Subsequent studies will investigate more homogeneous patient populations.

CONCLUSIONS

We successfully used ^{68}Ga-RM2 in a prospective study that enrolled patients with BCR PCa and negative CI. High focal uptake in putative and biopsy-proven sites of recurrent PCa in 23 of the 32 participants was observed using a TOF-enabled simultaneous PET/MRI. ^{68}Ga-RM2 PET can detect more lesions than MRI alone. Therefore, we propose ^{68}Ga-RM2 is a promising PET radiopharmaceutical for localization of disease in patients with BCR PCa and negative CI. Future work should explore its role in relationship to widely adopted PSMA PET radiopharmaceuticals such as ^{68}Ga PSMA-11.

ACKNOWLEDGEMENTS

We thank Dawn Banghart, George Segall and the other members of the RDRC for advice and support. We also thank our research coordinators Pam Gallant and Krithika Rupnarayan, the Cyclotron and Radiochemistry Facility, and the nuclear medicine technologists. Special thank you to all the patients who agreed to participate in the study and their families.

Precursor and reference compound were provided by Piramal Imaging, GmbH.

REFERENCES:

1. Isbarn H, Wanner M, Salomon G, et al. Long-term data on the survival of patients with prostate cancer treated with radical prostatectomy in the prostate-specific antigen era. *BJU Int.* 2010;106:37-43.

2. D'Amico AV, Whittington R, Malkowicz SB, et al. Pretreatment nomogram for prostate-specific antigen recurrence after radical prostatectomy or external-beam radiation therapy for clinically localized prostate cancer. *J Clin Oncol.* 1999;17:168-172.

3. Van Poppel H, Vekemans K, Da Pozzo L, et al. Radical prostatectomy for locally advanced prostate cancer: results of a feasibility study (EORTC 30001). *Eur J Cancer.* 2006;42:1062-1067.

4. Beer AJ, Eiber M, Souvatzoglou M, Schwaiger M, Krause BJ. Radionuclide and hybrid imaging of recurrent prostate cancer. *Lancet Oncol.* 2011;12:181-191.

5. Oyen RH, Van Poppel HP, Ameye FE, Van de Voorde WA, Baert AL, Baert LV. Lymph node staging of localized prostatic carcinoma with CT and CT-guided fine-needle aspiration biopsy: prospective study of 285 patients. *Radiology.* 1994;190:315-322.

6. Johnson LM, Turkbey B, Figg WD, Choyke PL. Multiparametric MRI in prostate cancer management. *Nat Rev Clin Oncol.* 2014;11:346-353.

7. Steiger P, Thoeny HC. Prostate MRI based on PI-RADS version 2: how we review and report. *Cancer Imaging.* 2016;16:9.

8. Le JD, Tan N, Shkolyar E, et al. Multifocality and prostate cancer detection by multiparametric magnetic resonance imaging: correlation with whole-mount histopathology. *Eur Urol.* 2015;67:569-576.

9. Priester A, Natarajan S, Khoshnoodi P, et al. Magnetic resonance imaging underestimation of prostate cancer geometry: use of patient specific molds to correlate images with whole mount pathology. *J Urol.* 2017;197:320-326.

10. Sonn GA, Chang E, Natarajan S, et al. Value of targeted prostate biopsy using magnetic resonance-ultrasound fusion in men with prior negative biopsy and elevated prostate-specific antigen. *Eur Urol.* 2014;65:809-815.

11. Sandblom G, Sorensen J, Lundin N, Haggman M, Malmstrom PU. Positron emission tomography with C11-acetate for tumor detection and localization in patients with prostate-specific antigen relapse after radical prostatectomy. *Urology.* 2006;67:996-1000.

12. Oyama N, Miller TR, Dehdashti F, et al. 11C-Acetate PET imaging of prostate cancer: detection of recurrent disease at PSA relapse. *J Nucl Med.* 2003;44:549-555.

13. Wachter S, Tomek S, Kurtaran A, et al. 11C-acetate positron emission tomography imaging and image fusion with computed tomography and magnetic resonance imaging in patients with recurrent prostate cancer. *J Clin Oncol.* 2006;24:2513-2519.

14. Eiber M, Maurer T, Souvatzoglou M, et al. Evaluation of hybrid 68Ga-PSMA ligand PET/CT in 248 patients with biochemical recurrence after radical prostatectomy. *J Nucl Med.* 2015;56:668-674.

15. Rowe SP, Gage KL, Faraj SF, et al. 18F-DCFBC PET/CT for PSMA-based detection and characterization of primary prostate cancer. *J Nucl Med.* 2015;56:1003-1010.

16. Sathekge M, Lengana T, Modiselle M, et al. 68Ga-PSMA-HBED-CC PET imaging in breast carcinoma patients. *Eur J Nucl Med Mol Imaging.* 2017;44:689-694.

17. Rhee H, Blazak J, Tham CM, et al. Pilot study: use of gallium-68 PSMA PET for detection of metastatic lesions in patients with renal tumour. *EJNMMI Res.* 2016;6:76.

18. Hermann RM, Djannatian M, Czech N, Nitsche M. Prostate-specific membrane antigen PET/CT: false-positive results due to sarcoidosis? *Case Rep Oncol.* 2016;9:457-463.

19. Sasikumar A, Joy A, Nanabala R, Pillai MR, T AH. 68Ga-PSMA PET/CT false-positive tracer uptake in Paget disease. *Clin Nucl Med.* 2016;41:e454-455.

20. Noto B, Vrachimis A, Schafers M, Stegger L, Rahbar K. Subacute stroke mimicking cerebral metastasis in 68Ga-PSMA-HBED-CC PET/CT. *Clin Nucl Med.* 2016;41:e449-451.

21. Jensen RT, Battey JF, Spindel ER, Benya RV. International Union of Pharmacology. LXVIII. Mammalian bombesin receptors: nomenclature, distribution, pharmacology, signaling, and functions in normal and disease states. *Pharmacol Rev.* 2008;60:1-42.

22. Reubi JC, Wenger S, Schmuckli-Maurer J, Schaer J-C, Gugger M. Bombesin receptor subtypes in human cancers: detection with the universal radioligand 125I-[d-TYR6, β-ALA11, PHE13, NLE14] Bombesin(6–14). *Clinical Cancer Research.* 2002;8:1139-1146.

23. Sun B, Halmos G, Schally AV, Wang X, Martinez M. Presence of receptors for bombesin/gastrin-releasing peptide and mRNA for three receptor subtypes in human prostate cancers. *Prostate.* 2000;42:295-303.

24. Markwalder R, Reubi JC. Gastrin-releasing peptide receptors in the human prostate: relation to neoplastic transformation. *Cancer Res.* 1999;59:1152-1159.

25. Minamimoto R, Hancock S, Schneider B, et al. Pilot comparison of 68Ga-RM2 PET and 68Ga-PSMA-11 PET in patients with biochemically recurrent prostate cancer. *J Nucl Med.* 2016;57:557-562.

26. Antoch G, Bockisch A. Combined PET/MRI: a new dimension in whole-body oncology imaging? *Eur J Nucl Med Mol Imaging.* 2009;36 Suppl 1:S113-120.

27. Cookson MS, Aus G, Burnett AL, et al. Variation in the definition of biochemical recurrence in patients treated for localized prostate cancer: the American Urological Association Prostate Guidelines for Localized Prostate Cancer Update Panel report and recommendations for a standard in the reporting of surgical outcomes. *J Urol.* 2007;177:540-545.

28. Roach M, 3rd, Hanks G, Thames H, Jr., et al. Defining biochemical failure following radiotherapy with or without hormonal therapy in men with clinically localized prostate cancer: recommendations of the RTOG-ASTRO Phoenix Consensus Conference. *Int J Radiat Oncol Biol Phys.* 2006;65:965-974.

29. Fendler WP, Eiber M, Beheshti M, et al. 68Ga-PSMA PET/CT: Joint EANM and SNMMI procedure guideline for prostate cancer imaging: version 1.0. *Eur J Nucl Med Mol Imaging.* 2017;44:1014-1024.

30. Iagaru A, Mittra E, Minamimoto R, et al. Simultaneous whole-body time-of-flight 18F-FDG PET/MRI: a pilot study comparing SUVmax with PET/CT and assessment of MR image quality. *Clin Nucl Med.* 2015;40:1-8.

31. Loening AM, Saranathan M, Ruangwattanapaisarn N, Litwiller DV, Shimakawa A, Vasanawala SS. Increased speed and image quality in single-shot fast spin echo imaging via variable refocusing flip angles. *J Magn Reson Imaging.* 2015;42:1747-1758.

32. Fanti S, Minozzi S, Morigi JJ, et al. Development of standardized image interpretation for 68Ga-PSMA PET/CT to detect prostate cancer recurrent lesions. *Eur J Nucl Med Mol Imaging.* 2017;44:1622-1635.

33. Roivainen A, Kahkonen E, Luoto P, et al. Plasma pharmacokinetics, whole-body distribution, metabolism, and radiation dosimetry of 68Ga bombesin antagonist BAY 86-7548 in healthy men. *J Nucl Med.* 2013;54:867-872.

34. Kahkonen E, Jambor I, Kemppainen J, et al. In vivo imaging of prostate cancer using [68Ga]-labeled bombesin analog BAY86-7548. *Clin Cancer Res.* 2013;19:5434-5443.

35. Nishino H, Tsunoda Y, Owyang C. Mammalian bombesin receptors are coupled to multiple signal transduction pathways in pancreatic acini. *Am J Physiol.* 1998;274:G525-534.

36. Polak JM, Bloom SR, Hobbs S, Solcia E, Pearse AG. Distribution of a bombesin-like peptide in human gastrointestinal tract. *Lancet.* 1976;1:1109-1110.

37. Erspamer V, Improta G, Melchiorri P, Sopranzi N. Evidence of cholecystokinin release by bombesin in the dog. *Br J Pharmacol.* 1974;52:227-232.

38. D'Amico AV, Renshaw AA, Sussman B, Chen MH. Pretreatment PSA velocity and risk of death from prostate cancer following external beam radiation therapy. *JAMA.* 2005;294:440-447.

39. Maina T, Bergsma H, Kulkarni HR, et al. Preclinical and first clinical experience with the gastrin-releasing peptide receptor-antagonist [68Ga]SB3 and PET/CT. *Eur J Nucl Med Mol Imaging.* 2016;43:964-973.

40. Dalm SU, Bakker IL, de Blois E, et al. 68Ga/177Lu-NeoBOMB1, a novel radiolabeled GRPR antagonist for theranostic use in oncology. *J Nucl Med.* 2017;58:293-299.

41. Nock BA, Kaloudi A, Lymperis E, et al. Theranostic perspectives in prostate cancer with the gastrin-releasing peptide receptor antagonist NeoBOMB1: preclinical and first clinical results. *J Nucl Med.* 2017;58:75-80.

42. Baratto L, Park SY, Hatami N, et al. 18F-FDG silicon photomultiplier PET/CT: a pilot study comparing semi-quantitative measurements with standard PET/CT. *PLoS One.* 2017;12:e0178936.

FIGURE CAPTIONS:

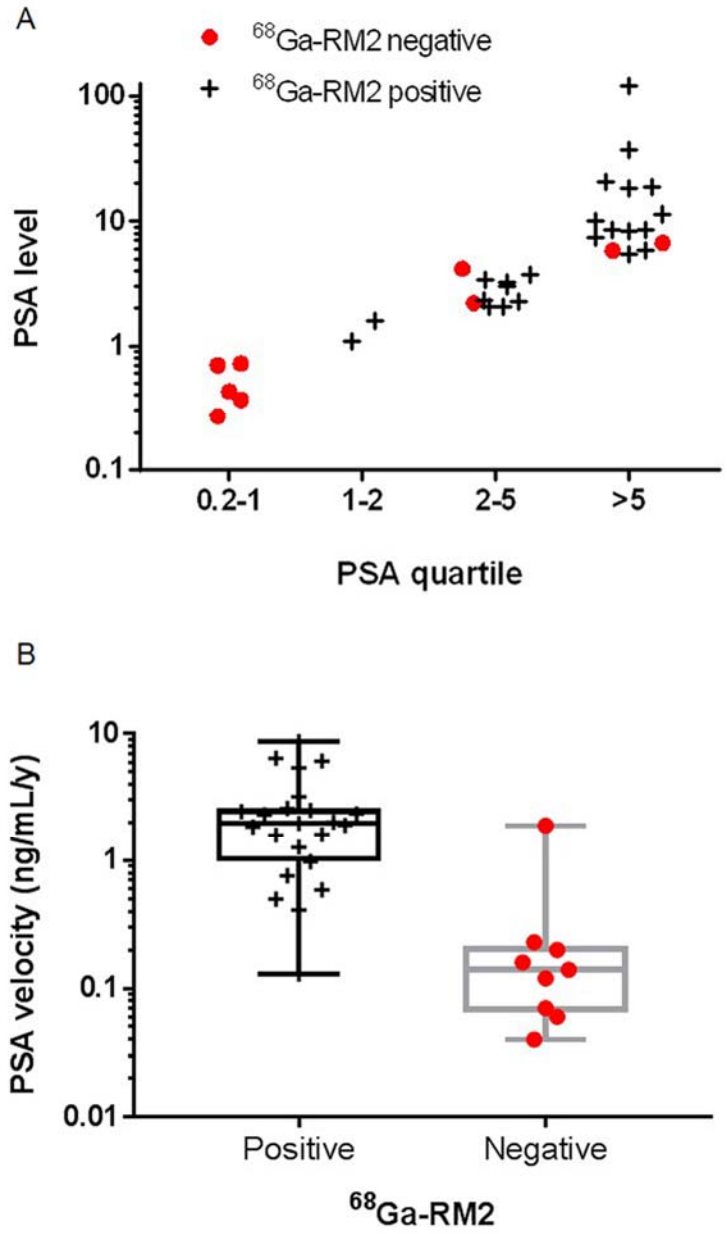

Figure 1: Relationship between results of ^{68}Ga-RM2 PET and A) PSA values (81% of patients with PSA > 1 ng/ml had positive scans) or B) PSAv.

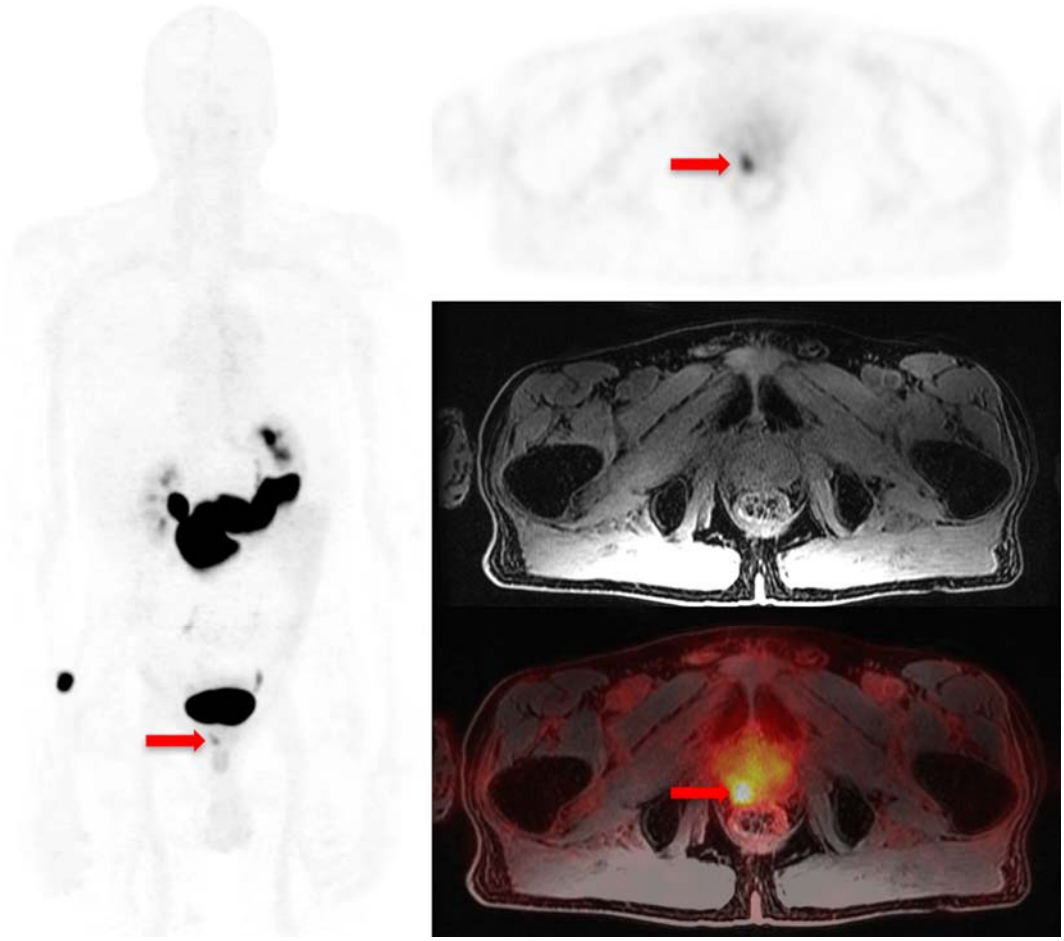

Figure 2: 72 year-old man (participant #6) with PCa treated with radiation therapy and androgen deprivation therapy at initial presentation (Gleason 3+4), now with BCR since 2013 and rising PSA (0.21 to 3.7 ng/ml at time of the scan). MIP and transaxial ^{68}Ga-RM2 PET images show focal uptake corresponding to the prostate bed on MRI (T1w) and fused PET/MRI. The focal uptake in the prostate bed was confirmed by biopsy to represent recurrent adenocarcinoma.

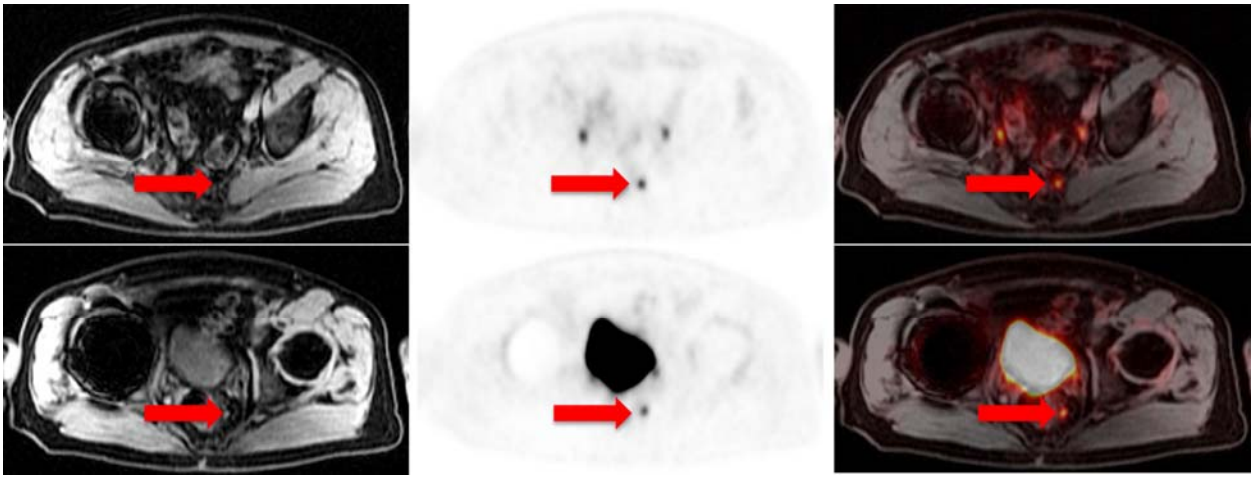

Figure 3: 65 year-old man (participant #11) with PCa treated with radical prostatectomy at initial presentation (Gleason 4+3), now with BCR since 2015 and rising PSA (from 0.45 to 2.33 ng/ml at time of the scan). Transaxial ^{68}Ga-RM2 PET images show focal uptake corresponding to sub-5 mm pelvic lymph nodes on MRI (T1w) and fused PET/MRI. PSA decreased to <0.05 ng/ml after pelvic radiation therapy targeting these lymph nodes.

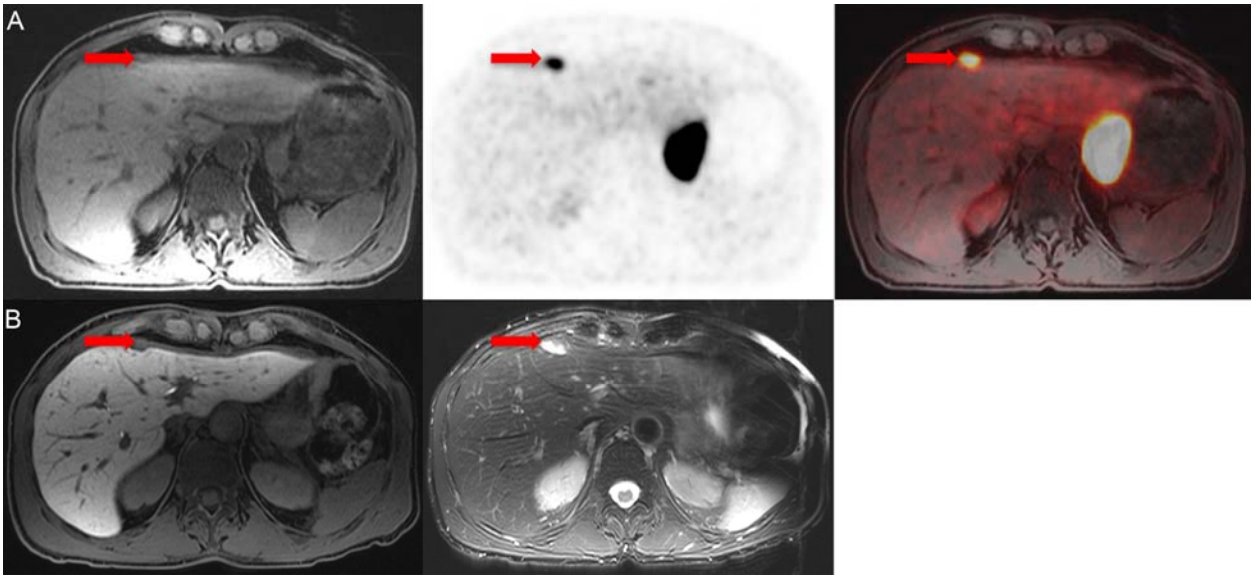

Figure 4: 65 year-old man (participant #23) with PCa treated with radical prostatectomy, radiation therapy and androgen blockade at initial presentation (Gleason 3+5), now with BCR since 2014 and rising PSA (from 0.72 to 3.4 ng/ml at time of the scan). (A) Transaxial ^{68}Ga-RM2 PET images show focal uptake corresponding the liver capsule on MRI (T1w) and fused PET/MRI. MRI did not identify an anatomical lesion. (B) Follow-up MRI done ***4 months later*** indicate a lesion that was biopsy-proven to represent metastatic adenocarcinoma of prostate origin.

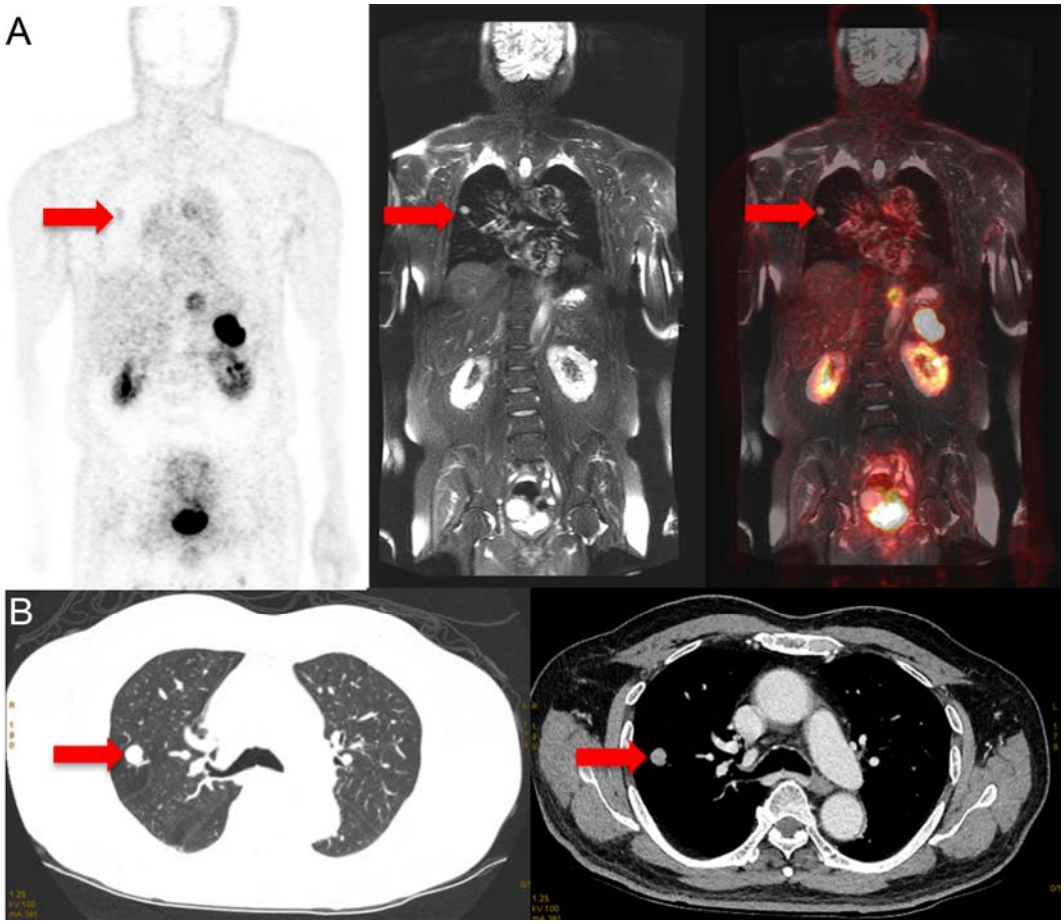

Figure 5: 66 year-old man (participant #20) with PCa treated with surgery, radiation therapy and androgen deprivation therapy at initial presentation (Gleason 5+4), now with BCR since 2010 and rising PSA (0.07 to 10.1 ng/ml at time of the scan). (A) Coronal ^{68}Ga-RM2 PET images show faint (but above adjacent normal lung parenchyma) focal uptake corresponding to a lung nodule on MRI (T2w) and fused PET/MRI. (B) Follow-up dedicated chest CT done ***2 weeks later*** demonstrates the lung nodule that was biopsy-proven to represent metastatic adenocarcinoma of prostate origin.

Supplemental Table 1: Patient characteristics

Patient No	Age	Height	Weight	Stage*	GS*	PSA nadir	PSA velocity**	PSA**	PSA to RM2 PET (days)	BCR to RM2 PET (months)	Conventional imaging**	Conventional imaging to RM2 PET (days)
1	83	5'4"	167	II	5+4	<0.05	6.45	18.7	3	40	CT A/P ^{18}F NaF PET/CT	45
2	69	5'6"	149	II	3+4	<0.05	2.45	8.6	1	5	MRI P ^{18}F NaF PET/CT	34
3	75	5'10"	189	IV	4+5	0.09	2.35	36.4	3	75	CT A/P ^{99m}Tc MDP bone scan	45
4	67	6'1"	243	II	3+3	0.14	0.23	6.7	14	51	CT A/P ^{99m}Tc MDP bone scan	45
5	72	6'0"	220	III	4+3	1.2	1.28	8.53	6	29	CT A/P ^{99m}Tc MDP bone scan	30
6	72	6'1"	170	II	3+4	0.5	1.91	3.70	3	28	CT A/P ^{99m}Tc MDP bone scan	10
7	60	6'2"	205	III	3+4	0.26	5.38	11.2	1	13	CT A/P ^{99m}Tc MDP bone scan	30
8	79	5'7"	151	I	3+3	0.53	1.86	5.33	3	14	MRI P ^{18}F NaF PET/CT	30
9	81	5'7"	172	I	3+4	<0.05	3.21	7.36	15	28	CT A/P ^{99m}Tc MDP bone scan	40
10	73	6'0"	209	III	4+4	<0.05	8.68	18.2	22	25	MRI A/P ^{18}F NaF PET/CT	45
11	65	5'10"	193	II	4+3	<0.05	0.76	2.33	30	11	MRI A/P ^{99m}Tc MDP bone scan	41

12	59	5'9"	194	II	3+3	0.17	0.06	0.27	24	12	CT P ^{99m}Tc MDP bone scan	11
13	70	5'9"	161	II	4+3	0.29	0.41	1.1	28	5	CT A/P ^{99m}Tc MDP bone scan	28
14	59	5'11"	220	IV	4+5	<0.05	0.59	2.07	30	1	CT C/A/P MRI P ^{99m}Tc MDP bone scan	30
15	69	5'6"	135	III	3+4	0.1	0.98	2.07	30	4	MRI P ^{99m}Tc MDP bone scan	7
16	66	5.7"	135	III	4+3	0.15	0.50	3.00	30	41	CT C/A/P MRI A/P ^{99m}Tc MDP bone scan	30
17	73	5'11"	178	II	3+4	0.1	1.90	4.15	30	12	CT C/A/P ^{99m}Tc MDP bone scan	45
18	66	5'5"	152	II	4+5	5.92	2.31	8.30	28	2	CT C/A/P ^{99m}Tc MDP bone scan	25
19	59	5'10"	190	II	4+4	2.65	2.50	3.25	21	3	CT A/P ^{99m}Tc MDP bone scan	22
20	66	5'4"	150	II	5+4	1.46	1.60	10.1	30	60	CT C/A/P ^{99m}Tc MDP bone scan	14
21	62	6'2"	215	II	4+3	0.2	0.14	0.72	3	65	CT A/P ^{99m}Tc MDP bone scan	17
22	59	5'9"	162	II	4+3	0.1	0.12	0.43	30	20	CT C/A/P ^{99m}Tc MDP bone scan	13
23	65	5'8"	125	III	3+4	<0.05	1.98	3.40	7	22	CT C/A/P ^{99m}Tc MDP bone scan	1

24	71	5'9"	190	II	3+4	0.1	0.20	5.80	30	20	CT C/A/P ^{99m}Tc MDP bone scan	29
25	63	6'0"	195	III	4+3	0.1	0.16	2.20	30	19	CT C/A/P MRI P ^{99m}Tc MDP bone scan	30
26	77	5'9"	174	III	5+5	0.3	6.10	119	30	24	CT A/P ^{99m}Tc MDP bone scan	30
27	67	6'1"	188	II	4+3	0.2	0.13	1.58	21	2	CT C/A/P ^{99m}Tc MDP bone scan	6
28	67	5'8"	186	III	4+5	<0.05	0.04	0.70	20	9	CT C/A/P ^{99m}Tc MDP bone scan	20
29	72	6'0"	183	IV	4+3	0.29	1.62	20.4	30	22	CT C/A/P ^{99m}Tc MDP bone scan	32
30	74	6'0"	210	II	4+4	<0.05	2.02	2.27	20	1	CT C/A/P ^{99m}Tc MDP bone scan	28
31	69	6'0"	270	II	4+3	<0.05	0.07	0.37	30	3	CT C/A/P ^{99m}Tc MDP bone scan	11
32	68	6’0”	193	II	5+3	<0.05	2.59	5.79	2	30	CT C/A/P ^{99m}Tc MDP bone scan	30

*: at initial diagnosis
**: at enrollment in the study
Gleason score: GS
Biochemical recurrence: BCR
Conventional imaging: CI
Chest: C
Abdomen: A
Pelvis: P

Supplemental Table 2: Prior treatments, results of the scans and follow-up

No	Treatment prior to enrolment	^{68}Ga-RM2 PET	MRI	F/U (months)	Treatment on F/U	Results of F/U	PET	MRI
1	HT+RT	Retroperitoneal LNs	Retroperitoneal LNs	25	Casodex and Lupron; RT to lymph nodes	MRI showed decreased size and number of retroperitoneal lymph nodes; PSA decreased from 18.7 to <0.05	TP	TP
2	Prostatectomy	Retroperitoneal LNs	Negative	24	Lupron; RT to lymph nodes	PSA initially increased from 8.6 to 10.9 on watch and wait, then decreased to <0.05 after treatment	TP	FN
3	Prostatectomy	Retroperitoneal LNs, pelvis soft tissue mass	Negative	24	Casodex and Lupron	CT showed decrease in size of soft tissue mass and LNs; PSA decreased from 36.4 to 0.27	TP	FN
4	Brachytherapy + HT	Negative	Negative	24	RT to right vas deferens	PSA increased from 6.7 to 12.1; biopsy results: 12 cores negative; right vas deferens showed 4+3; PSA decreased to <0.01 after RT	FN	FN
5	HT+RT	Left supraclavicular LN	Negative	23	Active surveillance	PSA increased from 8.53 to 26.4; biopsy of left supraclavicular LN showed metastatic adenocarcinoma of prostate origin	TP	FN
6	RT	Prostate bed	Negative	24	Brachytherapy to right lobe of prostate	Prostate biopsy showed adenocarcinoma; PSA increased from 3.7 to 12.4 (brachytherapy failure)	TP	FN
7	RT + HT	Prostate (diffuse)	Negative	23	Salvage prostatectomy	Biopsy showed 4+3 (left lateral mid), 4+4 (left lateral apex), 4+4 (left medial mid), 4+4 (left medial apex), 3+3 (right medial mid); PSA decreased from 11.2 to 0.43	TP	FN
8	RT	Pelvic LNs	Negative	23	Casodex and Lupron	PSA increased from 5.33 to 18.3; F/U MRI showed enlarging LNs; PSA decreased to 0.06	TP	FN
9	Prostatectomy	Right seminal vesicle, right pelvic LN	Right pelvic LN	23	Casodex	PSA decreased from 7.36 to <0.05	TP	TP
10	Prostatectomy	C/T/L spine, ribs, pelvis, femora, humeri, mediastinal/retroperitoneal LNs	C/T/L spine, ribs, pelvis, femora, humeri, mediastinal/retroperitoneal LNs	23	Casodex and Lupron	MRI showed bone marrow metastases; PSA decreased from 18.2 to 4.51	TP	TP

11	Prostatectomy	Left pelvic LNs	Negative	19	RT to lymph nodes	PSA decreased from 2.33 to <0.05	TP	FN
12	Prostatectomy	Negative	Negative	17	No F/U available	No F/U available	N/A	N/A
13	Prostatectomy + HT	Prostate bed	Prostate bed	17	Lupron; RT to prostate bed	PSA decreased from 1.1 to <0.05	TP	TP
14	Prostatectomy + RT + HT	Mediastinal LNs	Mediastinal LNs	16	Casodex and Lupron	PSA increased from 2.08 to 5.35; CT showed enlarging mediastinal and hilar LNs; PSA decreased to 0.14	TP	TP
15	Prostatectomy	Right pelvic LN	Negative	16	RT to lymph nodes	PSA decreased from 2.07 to 1.06	TP	FN
16	Prostatectomy	Pelvic LNs	Negative	16	Declined treatment	PSA increased from 3.0 to 3.4	TP	FN
17	Prostatectomy + HT	Negative	Negative	16	RT to lymph nodes	PSA increased to 8.9 on wait and watch strategy; pelvic LNs on ^{68}Ga PSMA-11; PSA decreased to 4.5 after RT	FN	FN
18	Prostatectomy	Pelvic LNs	Pelvic LNs	17	Casodex and Lupron	PSA decreased to <0.05	TP	TP
19	Prostatectomy	Pelvic LNs	Pelvic LNs	15	Active surveillance	PSA increased from 3.25 to 7.9	TP	TP
20	Prostatectomy + RT + HT	Right lung	Right lung	15	Video-assisted thoracoscopic surgery (VATS)	PSA increased to 13.5; lung biopsy showed metastatic adenocarcinoma of prostate origin; PSA decreased to 0.015 after VATS	TP	TP
21	Prostatectomy + RT	Negative	Negative	15	Active surveillance	PSA stable at 0.72	TN	TN
22	Prostatectomy	Negative	Negative	14	Active surveillance	PSA stable at 0.66	TN	TN
23	Prostatectomy + RT + HT	Liver	Negative	14	Casodex and Lupron; RT to liver capsule lesion	MRI (4 months later) showed 1.3 x 0.4 cm lesion along the liver capsule; biopsy showed adenocarcinoma of prostate origin; PSA decreased to <0.01	TP	FN
24	Prostatectomy + RT + HT	Negative	Negative	14	Active surveillance	PSA increased from 5.8 to 25.63	FN	FN
25	Prostatectomy	Negative	Negative	14	Active surveillance	PSA increased from 2.2 to 4.9	FN	FN
26	RT + HT	Left supraclavicular, retroperitoneal LNs	Negative	14	Casodex and Lupron; RT to retroperitoneal lymph nodes	PSA decreased from 119 to 29.9	TP	FN

27	Prostatectomy	Right pelvic LN	Right pelvic LN	14	Lupron	PSA decreased from 1.58 to 1.1	TP	TP
28	Prostatectomy + RT + HT	Negative	Negative	13	Active surveillance	PSA increased from 0.7 to 1.08	FN	FN
29	RT + HT	Right inguinal LNs	Right inguinal LNs	12	RT to lymph nodes	Biopsy showed adenocarcinoma of prostate origin; PSA decreased from 20.4 to <0.008	TP	TP
30	Prostatectomy + RT	Left lung nodule	Left lung nodule	11	Casodex and Lupron	PSA increased from 2.27 to 5.78; nodule too small to biopsy; PSA decreased to 2.92 after starting Casodex and Lupron	TP	TP
31	Prostatectomy + RT	Negative	Negative	9	Active surveillance	PSA increased from 0.37 to 1.1	FN	FN
32	Prostatectomy + RT + HT	Retroperitoneal LNs	Negative	3	Casodex and Lupron	PSA decreased from 5.79 to 1.2	TP	FN

Radiation therapy: RT, Hormone therapy: HT, LN: lymph node; Follow-up: F/U; Not-available: N/A